The International Journal of Biochemistry & Cell Biology 42 (2010) 98–105

Contents lists available at ScienceDirect

The International Journal of Biochemistry & Cell Biology

journal homepage: www.elsevier.com/locate/biocel

Mammalian Ste20-like protein kinase 3 induces a caspase-independent apoptotic pathway

Chia-Ying Lin, Hung-Yi Wu, Pei-Ling Wang, Chiun-Jye Yuan*

Department of Biological Science and Technology, National Chiao Tung University, Hsinchu 300, Taiwan, ROC

ARTICLE INFO

Article history:
Received 2 April 2009
Received in revised form 4 September 2009
Accepted 21 September 2009
Available online 25 September 2009

Keywords:
Mst3
Apoptosis
AIF
Endonuclease G
Mitochondria
DNase

ABSTRACT

In this study, it was shown that the mammalian sterile 20-like serine/threonine protein kinase 3 (Mst3) plays an essential role in the staurosporine-induced apoptosis of HeLa cells. The staurosporine-induced apoptosis was reduced by around 65% by the selective knockdown of Mst3 in stable clones, HeLa(siMst3). Although caspases were shown to be involved in the Mst3-mediated apoptosis, only 15–20% of staurosporine-induced apoptosis was suppressed by the caspase inhibitor, z-DEVD-fmk. Accordingly, Mst3 was proposed to trigger a caspase-independent apoptotic pathway in response to staurosporine. Interestingly, staurosporine greatly induced the mitochondrial membrane potential transition in HeLa cells, but had no effect in Hela(siMst3). The role of Mst3 in controlling the mitochondrial integrity was therefore proposed, presumably through the regulation of Bax. Furthermore, it was shown that staurosporine promoted the nuclear translocation of apoptosis-inducing factor and endonuclease G in HeLa cells. The nuclease activity associated with endonuclease G was also enhanced in response to staurosporine. However, both staurosporine-induced nuclear translocation of apoptosis-inducing factor and endonuclease G and the nuclease activity associated with endonuclease G were markedly reduced in Hela(siMst3). These results suggest that Mst3 may respond to staurosporine to trigger the caspase-independent apoptotic pathway by regulating the nuclear translocation of apoptosis-inducing factor and endonuclease G, and the nuclease activity associated with endonuclease G.

1. Introduction

Mammalian sterile 20-like serine/threonine protein kinase 3 (Mst3) is a 47.5 kDa human serine/threonine protein kinase belonging to a family of mammalian Ste20-like protein kinases found to regulate various cellular events in response to environmental cues (Bagrodia and Cerione, 1999; Huang et al., 2002; Kyriakis, 1999; Schinkmann and Blenis, 1997; Sells and Chernoff, 1997). Several studies have shown that Mst3 may play important roles in diverse physiological events (Huang et al., 2002; Irwin et al., 2006; Lee et al., 2004; Lu et al., 2006; Stegert et al., 2005). NDR, a serine/threonine protein kinase, is phosphorylated by Mst3 at Thr442 and this regulates cell cycle progression and cell morphology (Stegert et al., 2005). Additionally, Mst3 can control the migration of MCF-7 and Madin–Darby canine kidney cells by mediating the phosphorylation of paxillin (Lu et al., 2006). The neuron-specific Mst3b plays a role in regulating axonal outgrowth in a purine-dependent manner (Irwin et al., 2006). Interestingly, overexpression of Mst3 induces apoptotic characteristics, such as chromosome condensation and DNA fragmentation (Huang et al., 2002; Lee et al., 2004). Recent work has also demonstrated that Mst3 triggers apoptosis in human trophoblasts under conditions of oxidative stress and may play a role in parturition (Wu et al., 2008).

Apoptosis is a fundamental and indispensable process that serves to eliminate excess cells during tissue homeostasis (Clarke, 1990), embryonic development (Glucksmann, 1951; Michaelson, 1987) and maturation of the immune system (Cohen et al., 1992; Golstein et al., 1991). Caspases, a family of aspartic acid-specific cysteine proteases, play essential roles in apoptosis to cleave various targets to inactivate normal cellular functions, inhibit anti-apoptotic mechanisms, disrupt cellular architecture and eventually cause cell death (Chang and Yang, 2000; Srinivasula et al., 1998). However, in many cases, apoptotic cell death can be induced independent of caspase activity through mitochondrial pro-apoptotic proteins (Cande et al., 2002; Danial and Korsmeyer, 2004; Ishihara and Shimamoto, 2006; Joza et al., 2001; Li et al., 2001; Newmeyer and Ferguson-Miller, 2003). During apoptosis, the integrity of the outer mitochondrial membrane can be disrupted by the activation of pro-apoptotic Bcl-2 family members (Godlewski et al., 2001; Kuwana et al., 2002; Luo et al., 1998; Martinou and Green, 2001;

Abbreviations: Mst3, mammalian Ste20-like protein kinase 3; AIF, apoptosis-inducing factor; EndoG, endonuclease G; DNase, deoxyribonuclease; TUNEL, terminal deoxynucleotidyltransferase-mediated nick end labeling; Sts, staurosporine; siRNA, small-interfering RNA.

* Corresponding author. Tel.: +886 3 5731735; fax: +886 5729288.
E-mail address: cjyuan@mail.nctu.edu.tw (C.-J. Yuan).

1357-2725/$ – see front matter © 2009 Elsevier Ltd. All rights reserved.
doi:10.1016/j.biocel.2009.09.012

Wolter et al., 1997) or by increased opening of permeable transition pores (Crompton, 1999). Altering the permeability of the outer mitochondrial membrane causes the release of cytochrome *C* (Cyto *C*) and/or other pro-apoptotic proteins, such as apoptotic-inducing factor (AIF) (Cande et al., 2002; Cheung et al., 2006; Joza et al., 2001; Susin et al., 1999; Zanna et al., 2005), endonuclease G (EndoG) (Hamada et al., 2006; Ishihara and Shimamoto, 2006; Lee et al., 2005; Li et al., 2001; Parrish et al., 2001; Zanna et al., 2005; Zhang et al., 2003), Smac/DIABLO (Adrain et al., 2001), the mammalian serine protease Omi/HtrA2 (Suzuki et al., 2001; Verhagen et al., 2002) and DNA fragmentation factor endonuclease (DFF40) (Widlak et al., 2000). Subsequently, pro-apoptotic proteins, including AIF and EndoG, may translocate to the nucleus, where they trigger chromosome condensation and DNA fragmentation.

In this report, Mst3 was found to play an essential role in staurosporine-induced apoptosis by triggering both caspase-dependent and -independent pathways. Further studies show that Mst3 may trigger a caspase-independent apoptotic pathway by regulating the nuclear translocation of AIF and EndoG and the DNase activity associated with EndoG.

2. Materials and methods

2.1. Materials

Restriction enzymes were obtained from New England BioLabs. Fetal bovine serum (FBS), Dulbecco's modified eagle medium (DMEM), penicillin G, streptomycin, and lipofectamine were obtained from Life Technologies. Staurosporine was bought from Sigma. Oligonucleotides were synthesized by BioBasic Inc., UK. SP600125 and z-DEVD-fmk, caspase inhibitor, were bought from Calbiochem. Other reagents used were reagent grade.

2.2. Cell culture and apoptosis analysis

Human cervical cancer cell line (HeLa) was maintained in DMEM containing 10% FBS and 100 U/mL penicillin and 100 μg/mL streptomycin. Cells were incubated in a humidified 37 °C incubation chamber containing 5% CO_2.

The terminal deoxynucleotidyl transferase (TdT)-mediated nick end labeling (TUNEL) assay was carried out by using Dead End™ Fluorometric TUNEL system kit (Promega). HeLa cells (5×10^6 cells) before and after treatment were collected by scraping from 100 mm dished and washed once with 1× PBS (phosphate-buffered saline). Cells were then resuspended in 1× PBS buffer and fixed with 0.1% formaldehyde for 10 min. After fixation, cells were rinsed three times with 1× PBS and then suspended in 5 mL ice-cold 70% ethanol. After incubating at −20 °C for at least 4 h, cells were collected and rinsed three times with PBS, followed by equilibrating with 100 μL equilibration buffer (10 mM Tris–HCl, pH 7.5 containing 10 mM EDTA and 10 mM DTT) at room temperature for 10 min. Finally, cells were incubated with TUNEL mix, which was composed of 1 μL TdT enzyme, 5 μL nucleotide mix (100 μM dATP, 50 μM FITC-12-dUTP, 1 mM EDTA, 10 mM Tris–HCl, pH 7.6) and 45 μL equilibration buffer, at 37 °C for 1 h. A negative control was prepared by omitting TdT. DNase I-treated slides were used as the positive control. The reaction was terminated by adding 1 mL 20 mM EDTA into the reaction mixture. Cells were then rinsed twice with 1× PBS and soaked in 1× PBS for flow cytometry analysis (CyFlow® SL, Partec).

For annexin V binding assay, cells were collected from 100 mm dishes and washed twice with cold 1× PBS. Subsequently, cells were resuspended in 500 μL of 1× binding buffer (0.01 M Hepes/NaOH buffer, pH 7.4 containing 0.14 M NaCl, 2.5 mM $CaCl_2$) and stained with 5 μL of annexin V-FITC and 5 μL of propidium iodide (50 μg/mL). After incubated at room temperature for 5 min in the dark, number of cells bound annexin V-FITC was analyzed on the flow cytometry.

2.3. Selective knockdown of endogenous Mst3 by siRNA

The construction of pNEO/siMst3 vector for the generation of siRNA of Mst3 (siMst3) was described previously (Wu et al., 2008). The pNEO/siMst3 plasmid was transfected into HeLa cells by lipofectamine transfection kit (Invitrogen). Five stable clones were generated under the selection of G418-sulfate. The efficacy of siRNA was determined by Western blotting with anti-Mst3 antibody to monitor the expression of Mst3 in HeLa stable clones.

2.4. Immunofluorescent staining

HeLa cells were cultured on a glass cover slide to about 70% confluency, followed by treating with or without 100 nM staurosporine at 37 °C for 8 h. After treatment, cells were fixed with 3.7% paraformaldehyde in 1× PBS at 4 °C for 20 min. Cells were then permeabilized with digitonin 2 mg/mL under room temperature for 10 min. After permeabilization, cells were blocked with 5% BSA under room temperature for 1 h, followed by incubating with 100 μL primary antibody specifically against AIF (Santa Cruz; 1:200 dilution in 1× PBS) or EndoG (Biovision; 1:200 dilution in 1× PBS) under the room temperature for 2 h. Following the incubation, cells were washed three times with PBST (phosphate-buffered saline, pH 7.4, 0.05% tween-20) and then incubated with fluorescence-conjugated secondary antibody (Santa Cruz; 1:100 dilution in 1× PBS) at room temperature for about 1 h in the dark. Mitochondria and nucleus were stained by Mitotracker (red fluorescence, Molecular Probe) and DAPI (blue fluorescence), respectively. Finally, cells were washed three times with PBST and once with double-deionized H_2O. Slides were mounted and sealed by nail polish. The fluorescent images were obtained using a confocal laser scanning microscope (FV500, Olympus, Japan) and processed using supplied software Fluoview.

2.5. Subcellular fractionation

Mitochondrial and nuclear fractions were prepared as described previously with some modification (An et al., 2004; Ito et al., 2001). Briefly, HeLa cells were initially suspended in 200 μL buffer I (10 mM Tris–HCl, pH 7.9, 10 mM KCl, 0.1 mM EDTA, 0.1 mM EGTA and 1 mM DTT) and incubated on ice for 15 min. After incubation, cells were homogenized by pressing cell suspension through a 26G syringe needle for six times. Cell lysate was then centrifuged at 1500 × *g* for 5 min to remove intact cells. The supernatant was then centrifuged at 3300 × *g* for 5 min to collect the nuclei. The remaining supernatant was then centrifuged at 7500 × *g* for 5 min to remove the undissolved particulates, followed by centrifugating at 22,065 × *g* for 30 min (Beckman, Allegra 21R) to collect mitochondria. Mitochondria were disrupted by incubating in 100 μL RIPA buffer (1% Triton X-100, 0.1% SDS, 50 mM Tris, pH 8.0,150 mM NaCl, 1 mM EDTA, 1 mM EGTA, 1% sodium deoxycholate, 0.1 μM leupeptin, and 0.03 μM aprotinin) on ice for 10 min. After centrifugation at 16,100 × *g* for 10 min, the soluble mitochondrial fraction was collected for further usage. For preparation of nuclear fraction, the collected nuclei were first washed three times with buffer I containing 0.01% NP-40 and then resuspended in RIPA buffer. The nuclei were disrupted by vigorous votexing at 4 °C for 15 min. After centrifugation at 16,100 × *g* for 10 min, the soluble nuclear fraction was collected for further usage.

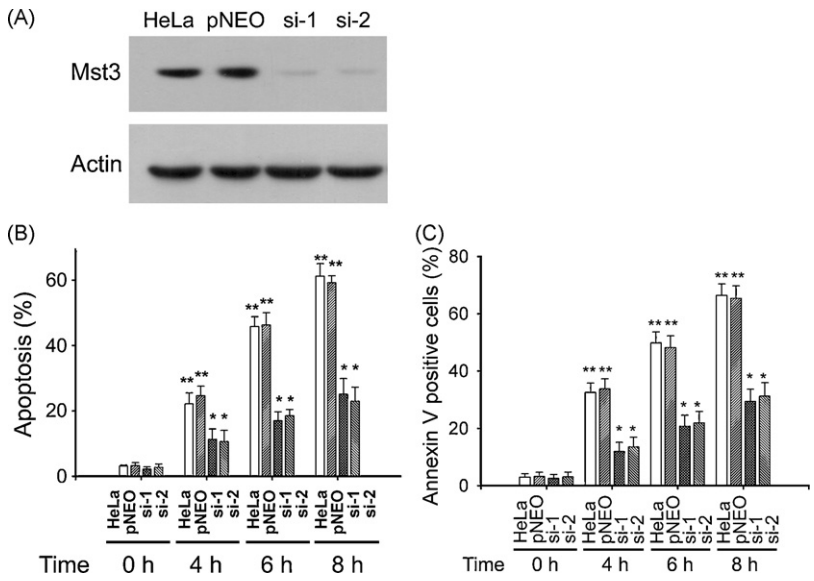

Fig. 1. Staurosporine-induced apoptosis can be suppressed by selective knockdown of Mst3. (A) Selective knockdown of Mst3 by siRNA in HeLa cells. Whole cell extracts from HeLa(siMst3)-1 and -2 clones (si-1 and si-2) were prepared and analyzed by Western blotting with anti-Mst3 antibody. HeLa cells and the HeLa(pNEO) clone (pNEO) were used as controls. (B) Staurosporine-induced apoptosis was inhibited in HeLa(siMst3)-1 and -2 clones. HeLa, HeLa(pNEO) (pNEO), HeLa(siMst3)-1 (si-1) and -2 (si-2) cells were treated with 100 nM staurosporine at 37 °C for 0, 4, 6 and 8 h, and then subjected to the TUNEL assay. Data are presented as mean ± S.D. from at least three independent experiments. $^{**}P < 0.01$ versus untreated cells at time 0 and $^{*}P < 0.01$ versus controls at each time point. (C) Staurosporine-induced annexin V binding was inhibited in HeLa(siMst3)-1 and -2 clones. HeLa, HeLa(pNEO) (pNEO), HeLa(siMst3)-1 (si-1) and -2 (si-2) cells were treated with 100 nM staurosporine at 37 °C for 0, 4, 6 and 8 h, and then subjected to the annexin V binding analysis. Data are presented as mean ± S.D. from at least three independent experiments. $^{**}P < 0.01$ versus untreated cells at time 0 and $^{*}P < 0.01$ versus controls at each time point.

2.6. Western blotting

Cell lysates (40 μg) or subcellular fractions (40 μg) were separated on a 10% SDS-polyacrylamide electrophoresis gel (SDS-PAGE). Following electrophoresis, the protein bands were transferred to a polyvinylidine difluoride (PVDF) membrane by electroblotting. The Western blot analysis was performed by using antibody specifically against Mst3 (BD Biosciences; 1:1000 dilution), caspase 3 (1:2000 dilution, Santa Cruz), active caspase 3 (1:2000 dilution, Santa Cruz), JNK1 (c-Jun N-terminal protein kinase 1) (1:2000 dilution, Santa Cruz), p-JNK1 (phosphorylated JMK1) (1:2000 dilution, Biovision), AIF (Epitomics;1:1000 dilution), EndoG (Biovision;1:1000 dilution) and Bax (Biosource; 1:1000 dilution). The protein bands were visualized using an ECL chemiluminescence kit. The β-actin (Santa Cruz; dilution 1:1000), Hsp60 (Santa Cruz; 1:1000 dilution), calnexin (Santa Cruz; 1:2000 dilution), GM130 (Santa Cruz; 1:1000 dilution), α-tubulin (Santa Cruz; 1:2000 dilution) and lamin B (Santa Cruz; 1:2000 dilution) were also used as internal controls for some experiments.

2.7. Immunoprecipitation and DNase activity assay

HeLa, HeLa(pNEO) and HeLa(siMst3) cells were treated with or without 100 nM staurosporine at 37 °C for 8 h. Total cell lysate without nuclear fraction was prepared by resuspending and incubating cells in 200 μL buffer I on ice for 15 min. Following incubation, cells were homogenized with a 26G syringe and then centrifuged at 3300 × *g* for 5 min. The supernatant without nuclei (1.5 mg) was then subjected to immunoprecipitation by incubating with 1.6 μg rabbit monoclonal antibody (Biovision) specific against EndoG or 1.6 μg mouse monoclonal antibody (Santa Cruz) specifically against AIF at 4 °C for 4 h. The 90% of total immunoprecipitate was then subjected to DNase assay. The rest immunoprecipitated proteins (about 10% of total immunoprecipitate) were used to determine the presence of EndoG by Western blotting.

The DNase activity associated with immunoprecipitate of EndoG antibody was detected by the cleavage of circular plasmid (Wang et al., 2002; Ye et al., 2002). The assay was performed by incubating immunoprecipitate with 1 μg pcDNA3.0 (5.4 kb) in a buffer containing 10 mM Tris–HCl, pH 7.5, 1 mM $MgCl_2$, 10 mM KCl, 0.1 mM PMSF and 1 mM DTT at 37 °C for 45 min. The reaction mixtures were then resolved and analyzed on a 1% agarose gel.

2.8. Determination of mitochondrial membrane depolarization ($\Delta\psi_m$)

The loss of $\Delta\psi_m$ was monitored with the dye 5,5′,6,6′-tetrachloro-1,1′,3,3′- tetraethylbenzimidazolyl-carbocyanine iodide (JC-1) (Cossarizza et al., 1993). The ratio between green and red fluorescence provides an estimate of $\Delta\psi_m$ that is independent of the mitochondrial mass. Briefly, HeLa, HeLa(pNEO) and HeLa(siMst3) cells (1×10^6 cells/mL) in 10-cm culture dishes were treated without or with 100 nM staurosporine for 0, 4 and 8 h. Cells were trypsinized, washed in ice-cold 1× PBS, and incubated with 10 μM JC-1 at 37 °C for 20 min in dark. After washing twice with 1× PBS, cells were analyzed on the flow cytometry (CyFlow® SL, Partec).

3. Results and discussion

3.1. Mst3 is essential in drug-induced apoptosis

Staurosporine is a pro-apoptotic drug derived from *Streptomyces staurospores* that induces apoptosis in HeLa cells, possibly in an Mst3-dependent manner (Huang et al., 2002). The role of Mst3 in staurosporine-induced apoptosis was investigated by selective knockdown of Mst3 in HeLa cells. Two of the five stable clones generated, HeLa(siMst3)-1 and -2, were used in the study. Endogenous Mst3 protein levels were reduced by at least 70% in the stable clones (Fig. 1A). The level of HeLa cell apoptosis induced by staurosporine was determined by DNA fragmentation and found to be time-dependent. When HeLa cells were treated with 100 nM of staurosporine, apoptosis levels increased from 3.13 ± 0.31% at 0 h to 22.1 ± 3.4%, 45.8 ± 3.0% and 61.2 ± 3.8% at 4, 6 and 8 h of treatment, respectively (Fig. 1B). Similar results were also observed in

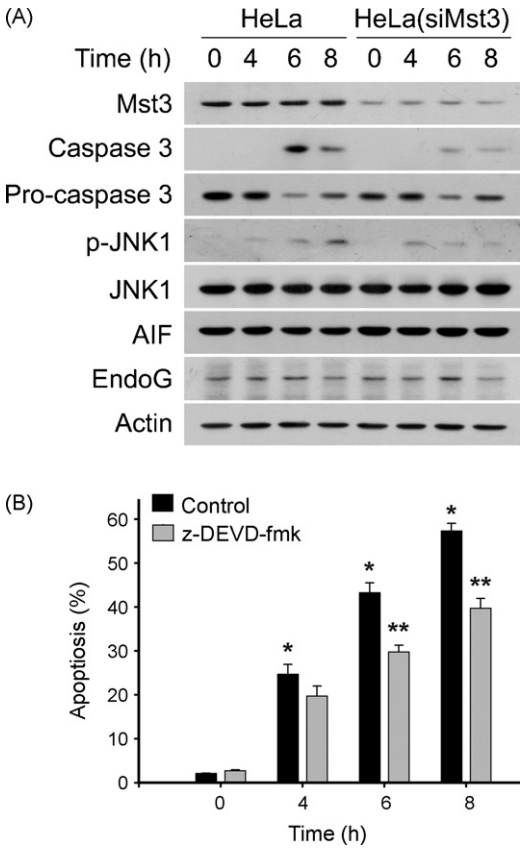

Fig. 2. The role of caspase 3 in staurosporine-induced apoptosis. (A) Effect of Mst3 knockdown on the activation of caspase 3 and JNK. HeLa cells and HeLa(siMst3)-1 clone were treated with 100 nM staurosporine at 37 °C for 0, 4, 6 and 8 h. Cell lysates were then separated on 10% SDS-PAGE and probed with antibodies against Mst3, active caspase 3, pro-caspae 3, JNK, p-JNK, AIF and EndoG. Actin was used as a loading control. (B) HeLa cells (5×10^6 cells) in 100 mm culture plates were pre-treated with 50 μM z-DEVD-fmk at 37 °C for 30 min, followed by treatment with 100 nM staurosporine at 37 °C for 0, 4, 6 and 8 h. After incubation, cells were subjected to the TUNEL assay. Data are presented as mean ± S.D. from at least three independent experiments. *$P < 0.01$ versus untreated cells at time 0 and **$P < 0.05$ versus cells without z-DEVD-fmk at each time point.

the HeLa(pNEO) clone after treatment (Fig. 1B, pNEO). Compared to controls, staurosporine-induced apoptosis was suppressed 52–63% in the Mst3 knockdown stable clones (Fig. 1B, si-1 and si-2).

The role of Mst3 in the staurosporine-induced apoptosis of HeLa cells was further investigated by measuring the exposure of phosphatidylserine (PS) on the outer leaflet of plasma membranes during early apoptosis (Savill and Haslett, 1995). The percentage of annexin V positive cells in HeLa cells increased from 3.0 ± 1.2% at 0 h to 32.5 ± 3.3%, 49.8 ± 3.8% and 66.4 ± 4.0% at 4, 6 and 8 h of treatment with staurosporine, respectively (Fig. 1C). Similar results were also observed in the HeLa(pNEO) clone. The staurosporine-induced PS exposure in the Mst3 knockdown stable clones was suppressed by 56–64% (Fig. 1B, si-1 and si-2). These results are similar to those observed in the TUNEL assay (Fig. 1C) and demonstrate that Mst3 is essential in staurosporine-induced apoptosis.

3.2. Moderate role of caspase in staurosporine-induced apoptosis

Previously, caspases were shown to play a role in the Mst3-mediated apoptosis (Huang et al., 2002; Wu et al., 2008). In HeLa cells, the levels of active caspase 3 increased after 6 h of staurosporine treatment and declined slightly after 8 h (Fig. 2A). Interestingly, it was found that the staurosporine-induced caspase 3 activation was partially reduced by the selective knockdown of Mst3 in the stable HeLa(siMst3) clone (Fig. 2A). This suggests a role of Mst3 in regulating the activity of caspase 3 in HeLa cells. Furthermore it was found that the staurosporine-induced apoptosis of HeLa cells was only moderately reduced (15–20%) by the treatment of caspase 3 inhibitor, z-DEVD-fmk (Fig. 2B). In the presence of 50 μM z-DEVD-fmk, the staurosporine-induced apoptosis of HeLa cells decreased from 24.7 ± 2.3% to 19.7 ± 2.3% at 4 h, from 43.3 ± 2.3% to 29.8 ± 1.5% at 6 h and from 57.3 ± 1.7% to 39.7 ± 2.4% at 8 h. These results indicate that caspase 3 plays a minor role in Mst3-mediated apoptosis and that its activation is in response to staurosporine. It was also postulated that a caspase-independent pathway could be activated by Mst3, blocking the further activation of caspase 3. In addition, Mst3 was postulated to be further activated by the active caspase 3-mediated proteolytic cleavage of its C-terminus (Huang et al., 2002). However, the presence of truncated forms of Mst3 in staurosporine-treated HeLa cells was not established due to the lack of antibodies that could specifically recognize the N-terminus of Mst3.

It was found that the c-Jun N-terminal protein kinase-1 (JNK1) was activated by staurosporine in a time-dependent manner (Fig. 2A). Interestingly, the staurosporine-induced activation of JNK1 was moderately suppressed by the selective knockdown of Mst3 in HeLa(siMst3) stable clone (Fig. 2A). These results suggest that Mst3 may play a role in the regulation of JNK1 however, how Mst3 mediates the activity JNK1 is currently unknown. Collectively, Mst3 can trigger both caspase-dependent and -independent apoptotic pathways in HeLa cells in response to staurosporine, though primarily a caspase-independent pathway.

Table 1
Induction of mitochondrial $\Delta\psi_m$ change in HeLa, HeLa(pNEO) and HeLa(siMst3) cells by staurosporine.

Time of staurosporine treatment (h)	Percentage of cells exhibiting red to green fluorescence transition[a]		
	HeLa	HeLa(pNEO)	HeLa(siMst3)
0	0.4 ± 0.5	0.9 ± 0.6	0.6 ± 0.5
4	32.1 ± 2.5	35.1 ± 2.9	5.8 ± 1.1
8	70.3 ± 3.5	73.6 ± 4.1	2.1 ± 0.8

[a] Mitochondrial $\Delta\psi_m$ change of HeLa, HeLa(pNEO) and HeLa(siMat3) cells was determined by flow cytometric analysis with JC-1 staining.

3.3. Mst3 controls the mitochondrial membrane permeability

Mitochondria house several key pro-apoptotic proteins essential for both caspase-dependent and -independent pathways. The disruption of the mitochondrial membrane and loss of mitochondrial membrane potential ($\Delta\psi_m$) during cell death has been indicated as one of the early events and a hallmark of apoptosis (Kuwana et al., 2002; Luo et al., 1998; Martinou and Green, 2001). To assess whether staurosporine affects the function of mitochondria, membrane potential transition (MPT) in mitochondria was analyzed by employing a mitochondrial fluorescent dye, JC-1, which is capable of selectively entering mitochondria. When $\Delta\psi_m$ is relatively low, JC-1 forms monomers and emits green fluorescence. At high $\Delta\psi_m$, JC-1 aggregates and emits red fluorescence (Cossarizza et al., 1993). Mitochondria in control cells primarily emitted a red/orange fluorescence. Once exposed to 100 nM staurosporine the MPT of control cultures, detected as green particles in JC-1 staining, significantly increased from 0.4 ± 0.5% at time 0 h, to 32.1 ± 2.5%, and 70.3 ± 3.5% at 4 and 8 h in HeLa cells, respectively (Fig. 3 and Table 1). Similar results were also observed in HeLa(pNEO) stable clone, a control cell with the pNEO plasmid only (Table 1). These results suggest that a significant MPT occurs in HeLa cells treated with 100 nM staurosporine. In contrast, the staurosporine-induced MPT was greatly suppressed in the stable

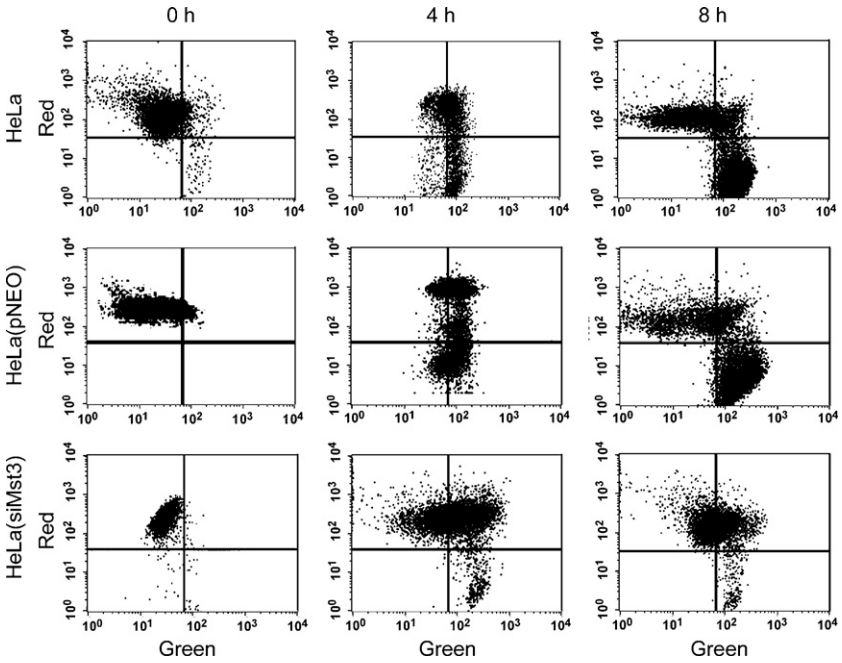

Fig. 3. Effect of Mst3 in mitochondrial membrane permeability. Analysis of $\Delta\psi_m$ in HeLa, HeLa(pNEO) and HeLa(siMst3) cells treated with 100 nM staurosporine was performed by flow cytometry. The transition of red fluorescence to green indicates mitochondrial membrane depolarization in cells. Total number of events analyzed for each condition was 10,000. The representative scattergrams from one of three independent experiments are presented.

HeLa(siMst3) clone (Fig. 3 and Table 1), with only $5.8 \pm 1.1\%$ and $2.1 \pm 0.8\%$ cells exhibiting MPT after 4 and 8 h of treatment, respectively. These results indicate that Mst3 may trigger apoptosis by altering the integrity of mitochondria.

Western blot analysis showed that the level of AIF and EndoG in HeLa and HeLa(siMst3) cells did not change significantly, even after treatment with staurosporine (Fig. 4A, whole cell; Fig. 4B, right panel). A slight decrease in the mitochondrial AIF content may indicate the release of AIF from mitochondria in response to staurosporine treatment (Fig. 4A, mitochondria). However, no change in the mitochondrial EndoG content was observed after staurosporine treatment. This may be due to the stringent washing process during the preparation of the mitochondrial fraction to avoid the contamination with other subcellular compartments. The purity of the isolated mitochondrial fraction was confirmed by the absence of the unique markers for other subcellular compartments, such as cytoplasm, nucleus, Golgi apparatus and endoplasmic reticulum in the Western blots (data not shown). In this case, most of damaged mitochondria might be disrupted and lost during the process of subcellular fractionation. Thus, the majority of the isolated mitochondria from the staurosporine-treated cells was intact and contained normal level of EndoG and AIF. Interestingly, the levels of AIF in the mitochondria of HeLa(siMst3) were moderately increased after staurosporine treatment (Fig. 4A, mitochondria). The reason for the mitochondrial AIF increase in HeLa(siMst3) after staurosporine treatment is unknown. AIF, a flavoprotein with NADH oxidase activity, is shown to play a role in supporting energy production in normal mitochondria (Cheung et al., 2006; Porter and Urbano, 2006). ATP has been shown to be required for the activation of caspases and apoptosis in response to staurosporine (Ferrari et al., 1998; Vier et al., 1999). Therefore, it is possible that the mitochondrial import of the cytosolic AIF (Daugas et al., 2000) is facilitated by staurosporine to compensate for the loss of healthy mitochondria, by which the ATP synthesis is reduced. In the HeLa(siMst3) stable clone, the release of mitochondrial AIF was suppressed by the selective knockdown of Mst3 and hence resulted in an increase of mitochondrial AIF levels in response to staurosporine.

Bax, a pro-apoptotic member of Bcl-2 family, has been shown to translocate from cytosol to mitochondria in response to staurosporine (Godlewski et al., 2001; Kuwana et al., 2002; Wolter et al., 1997). It also induces mitochondria permeabilization and the release of mitochondrial pro-apoptotic proteins. As expected, it was found that Bax was activated by staurosporine and translocated to the mitochondria in HeLa cells (Fig. 4A, mitochondria). The levels of Bax in the mitochondria increased about 4.6 folds, suggesting a role in staurosporine-induced apoptosis (Fig. 4B). However, in the stable HeLa(siMst3) clone, the expression of Bax reduced by about 65% compared with that in HeLa cells (Fig. 4A and B). This suggests a role of Mst3 in the regulation of Bax. This postulation was confirmed by the finding that the staurosporine-induced mitochondrial accumulation of Bax was greatly suppressed in HeLa(siMst3) cells (Fig. 4B). These results suggest that Mst3 may control the integrity of mitochondria and the release of mitochondrial pro-apoptotic proteins, presumably AIF and EndoG, by modulating the activity of Bax.

3.4. Role of Mst3 in staurosporine-induced nuclear translocation of AIF and EndoG

Mst3 was hypothesized to change the mitochondrial integrity in response to staurosporine and induce the nuclear translocation of AIF and EndoG. Without staurosporine treatment (−S), endogenous AIF and EndoG (green fluorescence) were found to colocalize with Mitotracker (red fluorescence), a mitochondrial specific fluorescent dye (yellow/orange signal; Fig. 5A and B). Controls with fluorescent probes conjugated to secondary antibodies exhibited only basal signals (data not shown). Further work showed that AIF (Fig. 5A) and EndoG (Fig. 5B) translocated to the nucleus in HeLa cells upon treatment with staurosporine (+S). Interestingly, when Mst3 was selectively knocked down in HeLa(siMst3) cells, the staurosporine-induced nuclear translocation of AIF (Fig. 5A) and EndoG (Fig. 5B) was blocked. The role of Mst3 in the nuclear translocation of AIF and EndoG was also demonstrated by subcellular fractionation and Western blot analysis. In HeLa cells, AIF and EndoG were found to accumulate in the nucleus upon treatment with staurosporine (Fig. 6, nuclear fraction). The absence of cal-

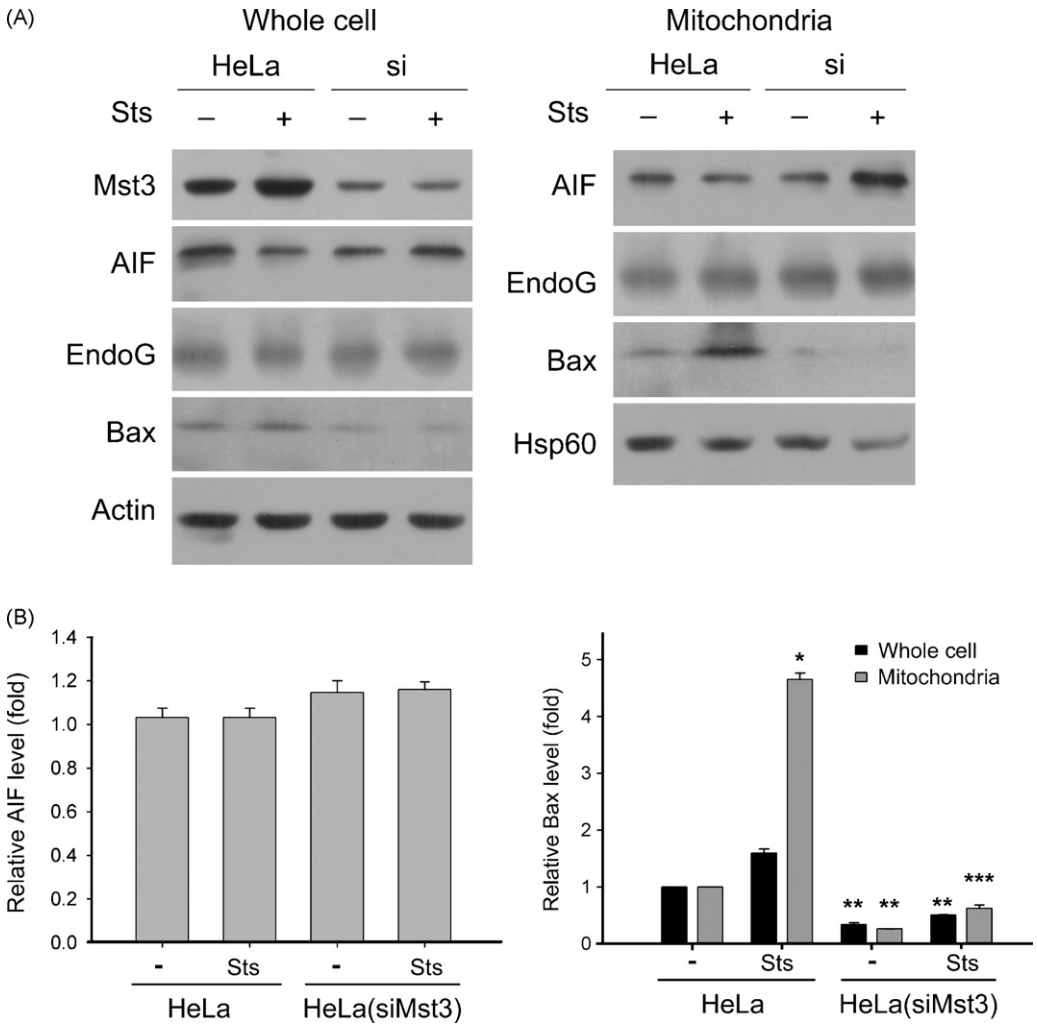

Fig. 4. Immunoblot analysis of mitochondrial pro-apoptotic proteins in HeLa and HeLa(siMst3) cells. (A) HeLa cells and HeLa(siMst3)-1 clone (si) were treated with or without 100 nM staurosporine (Sts) for 8 h. Whole cell extracts and mitochondrial fractions were separated on a 10% SDS-PAGE and probed with antibodies specifically against Mst3, AIF, EndoG and Bax. β-Actin and Hsp60 were used as internal controls of whole cell extract and mitochondrial fraction, respectively. (B) Quantitation of the AIF and Bax levels. (Left panel) AIF level in whole cell extract (whole cell panel in A) was quantitated by densitometry. (Right panel) Bax levels in whole cell extract and mitochondrial fraction were quantitated by densitometry. Both AIF and Bax levels in whole cell extract were normalized with the β-actin signal; while Bax in mitochondrial fraction was normalized with Hsp60 signal. $^{*}P < 0.01$ versus mitochondrial fraction from HeLa cells before staurosporine treatment, $^{**}P < 0.01$ versus whole cell extract or mitochondrial fraction from HeLa cells before staurosporine treatment and $^{***}P < 0.01$ versus mitochondrial faction from HeLa(siMst3) cells without treatment. Whole cell, whole cell extract; Mitochondria, mitochondrial fraction.

nexin, a specific marker of ER, and GM130, an unique marker of Golgi apparatus, in the isolated nuclear fractions indicated that the appearance of AIF and EndoG in nucleus of HeLa cells treated with staurosporine was not due to the contamination with ER and/or Golgi apparatus (Fig. 6). Consistent with previous results (Lee et al., 2004), Mst3 was also found in the nucleus after treatment with staurosporine. However, with selective knockdown of Mst3, the nuclear accumulation of AIF, EndoG and Mst3 in HeLa(siMst3) cells (si) was greatly reduced (Fig. 6, nuclear fraction). The expression of AIF and EndoG was not changed in the input controls (Fig. 6, whole cell extract). These results indicate that Mst3 plays an essential role in the staurosporine-induced nuclear translocation of AIF and EndoG.

3.5. Apoptotic DNA degradation is suppressed by selective knockdown of Mst3

It was shown that EndoG, an apoptotic DNase, was activated by apoptotic signals and promoted DNA fragmentation in a caspase-independent manner. However, the role of Mst3 in regulating the DNase activity of EndoG is unknown. Hence, the DNase activity of immunoprecipitated EndoG from HeLa, HeLa(pNEO) and HeLa(siMst3)-1 cells before and after staurosporine treatment was investigated by testing its ability to cleave an intact circular plasmid (Wang et al., 2002). On a 1% agarose gel, the intact pcDNA3.0 plasmid (C) exhibited two major bands (arrow and arrow head), and showed one band (asterisk) after HindIII cleavage (OC) (Fig. 7A). When incubating with immunoprecipitates from HeLa and HeLa(pNEO) without treatment, the pcDNA3.0 plasmid exhibited two major bands (arrow and asterisk) and one minor band (arrow head) as observed in lanes C and OC (Fig. 7A), suggesting the presence of a basal DNase activity in the immunoprecipitates. Upon treatment with staurosporine, however, the DNase activity associated with immunoprecipitates from HeLa and HeLa(pNEO) was markedly increased, evidenced by the reduction of the first band from top (arrow) and the disappearance of the middle band (arrow head). The appearance of smear in the lanes loaded with immunoprecipitates after staurosporine treatment also indicated an increase in DNase activity. Interestingly, this staurosporine-induced activation of DNase was greatly attenuated in the immunoprecipitates from HeLa(siMst3)-1 cells (Fig. 7A). Western blotting of EndoG immunoprecipitates (Fig. 7B) suggested

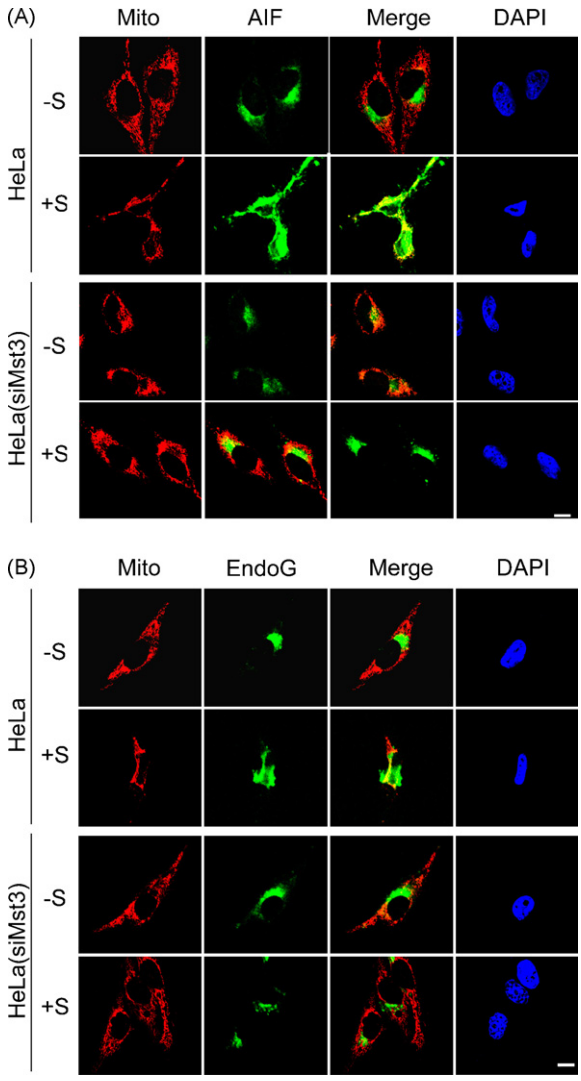

Fig. 5. Effect of Mst3 selective knockdown in the nuclear translocation of AIF and EndoG. Staurosporine-induced nuclear translocation of AIF (A) and EndoG (B) was demonstrated by immunofluorescent staining. HeLa or HeLa(siMst3) cells were treated with (+S) or without (−S) 100 nM staurosporine at 37 °C for 8 h. After treatment, cells were subjected to immunofluorescent staining. Representative fluorescent images from one of three independent experiments are presented.

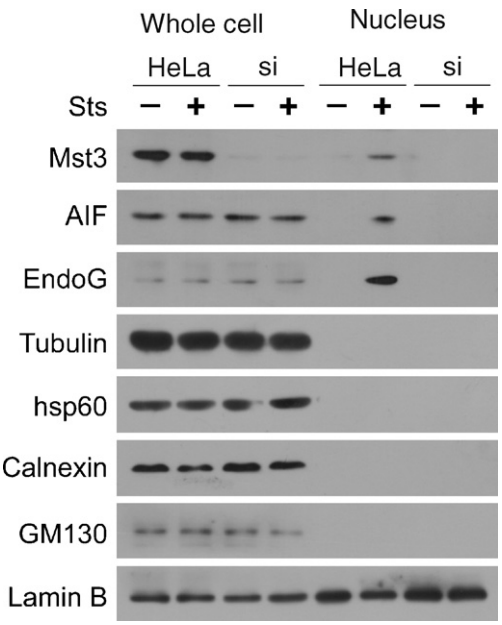

Fig. 6. Immunoblot analysis of the nuclear translocation of AIF and EndoG in HeLa and HeLa(siMst3) cells. HeLa, and HeLa(siMst3)-1 (si) cells were treated with or without 100 nM staurosporine (Sts) for 8 h. Whole cell extracts and nuclear fractions were prepared, separated on a 10% SDS-PAGE and probed with antibodies specifically against Mst3, AIF and EndoG. Calnexin, GM130, hsp60, α-tubulin and lamin B were used as internal controls for endoplasmic reticulum, Golgi apparatus, mitochondria, whole cell extract and nuclear fraction, respectively.

that the stimulatory effect of staurosporine and suppressive effect of selective knockdown of Mst3 on the DNase activity was not due to the differential input of immunoprecipitates. Previously, AIF was shown to associate with EndoG and promote DNase degradation and apoptosis (Wang et al., 2002). AIF was also proven to be co-immunoprecipitated with EndoG by Western blotting (Lin and Yuan, unpublished result). Similarly, the DNase activity associated with immunoprecipitates of AIF antibody could be enhanced by staurosporine treatment and suppressed by selective knockdown of Mst3 (data not shown). These results indicate that staurosporine-induced activation of DNase associated with EndoG and/or AIF depends on Mst3. However, the mechanism underlying the Mst3-mediated DNase activation is unknown.

Mst3 is a member of the GCK-III subfamily of human Ste20-like serine/threonine protein kinases previously suggested to play an essential role during drug- and oxidative stress-induced apoptosis (Huang et al., 2002; Wu et al., 2008). The involvement of caspase in Mst3-mediated apoptosis was demonstrated. Mst3 was shown in this study to trigger a caspase-independent apoptotic pathway, presumably through activating Bax that disrupts the integrity of mitochondria. Upon disruption of mitochondrial membrane, the residing AIF and EndoG, potent pro-apoptotic proteins, is then released from mitochondria and subsequently translocate to the nucleus. Interestingly, the staurosporine-induced nuclear translo-

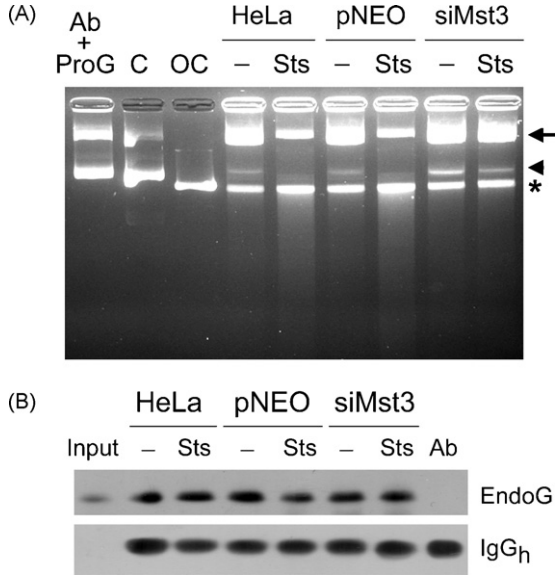

Fig. 7. Mst3 regulates the DNase activity associated with immunoprecipitates of EndoG antibody. (A) The EndoG antibody immunoprecipitates of cell lysates from HeLa, HeLa(pNEO) and HeLa(siMst3)-1 cells treated with or without 100 nM staurosporine (Sts) were prepared and subjected to DNase assay. Intact (C) and HindIII cleaved (OC) pcDNA3.0 plasmids were used as controls. HeLa, HeLa cells; pNEO, HeLa(pNEO) stable clone; siMst3, HeLa(siMst3) stable clone-1. Ab + ProG, EndoG antibody and protein G. Various DNA bands of pcDNA3.0 on agarose gel were indicated by arrow, arrow head and asterisk. Represented results are from one of three independent experiments. (B) Immunoblotting of immunoprecipitates with EndoG antibody from cell lysates of HeLa, HeLa(pNEO) and HeLa(siMst3)-1 cells. Input, input control (40 μg cell lysate); Ab, EndoG antibody only; IgG_h, IgG heavy chain.

cation of AIF and EndoG can be effectively suppressed by selective knockdown of Mst3, suggesting that this is a Mst3-dependent process. Furthermore, it was shown that the DNase activity associated with AIF and EndoG was regulated by Mst3 in the staurosporine-induced apoptotic pathway. In conclusion, Mst3 was found to play an important role in staurosporine-induced apoptosis by regulating both the nuclear translocation AIF and EndoG, as well as the DNase activity associated with them.

Acknowledgement

The authors would like to thank the National Science Council of the Republic of China, Taiwan, for financially supporting this research under Contract No. NSC-96-2311-B-009-001.

References

Adrain C, Creagh EM, Martin SJ. Apoptosis-associated release of Smac/DIABLO from mitochondria requires active caspases and is blocked by Bcl-2. EMBO J 2001;20:6627–36.
An J, Chen Y, Huang Z. Critical upstream signals of cytochrome *c* release induced by a novel Bcl-2 inhibitor. J Biol Chem 2004;279:19133–40.
Bagrodia S, Cerione RA. Pak to the future. Trends Cell Biol 1999;9:350–5.
Cande C, Cecconi F, Dessen P, Kroemer G. Apoptosis-inducing factor (AIF): key to the conserved caspase-independent pathways of cell death? J Cell Sci 2002;115:4727–34.
Chang HY, Yang X. Proteases for cell suicide: regulation and functions of caspases. Microbiol Mol Biol Rev 2000;64:821–46.
Cheung ECC, Joza N, Steenaart NAE, McClellan KA, Neuspiel M, McNamara S, et al. Dissociating the dual roles of apoptosis-inducing factor in maintaining mitochondrial structure and apoptosis. EMBO J 2006;25:4061–73.
Clarke PG. Developmental cell death: morphological diversity and multiple mechanisms. Anat Embryol (Berl) 1990;181:195–213.
Cohen JJ, Duke RC, Fadok VA, Sellins KS. Apoptosis and programmed cell death in immunity. Annu Rev Immunol 1992;10:267–93.
Cossarizza A, Baccarani CM, Kalashnikova G, Franceschi C. A new method for the cytofluorimetric analysis of mitochondrial membrane potential using the J-aggregate forming lipophilic cation 5,5′,6,6′-tetrachloro-1,1′,3,3′-tetraethylbenzimidazolcarbocyanine iodide (JC-1). Biochem Biophys Res Commun 1993;197:40–5.
Crompton M. The mitochondrial permeability transition pore and its role in cell death. Biochem J 1999;341:233–49.
Danial NN, Korsmeyer SJ. Cell death: critical control points. Cell 2004;116:205–19.
Daugas E, Nochy D, Ravagnan L, Loeffler M, Susin SA, Zamzami N, et al. Apoptosis-inducing factor (AIF): a ubiquitous mitochondrial oxidoreductase involved in apoptosis. FEBS Lett 2000;476:118–23.
Ferrari D, Stepczynska A, Los M, Wesselborg S, Schulze-Osthoff K. Differential regulation and ATP requirement for caspase-8 and caspase-3 activation during CD95- and anticancer drug-induced apoptosis. J Exp Med 1998;188:979–84.
Glucksmann A. Cell deaths in normal vertebrate ontogeny. Biol Rev Camb Philos Soc 1951;26:59–86.
Godlewski MM, Motyl MA, Gajkowska B, Wareski P, Koronkiewicz M, Motyl T. Subcellular redistribution of BAX during apoptosis induced by anticancer drugs. Anticancer Drugs 2001;12:607–17.
Golstein P, Ojcius DM, Young JD. Cell death mechanisms and the immune system. Immunol Rev 1991;121:29–65.
Hamada M, Sumi T, Iwai S, Nakazawa M, Yura Y. Induction of endonuclease G-mediated apoptosis in human oral squamous cell carcinoma cells by protein kinase C inhibitor safingol. Apoptosis 2006;11:47–56.
Huang CY, Wu YM, Hsu CY, Lee WS, Lai MD, Lu TJ, et al. Caspase activation of mammalian sterile 20-like kinase 3 (Mst3). J Biol Chem 2002;277:34367–74.
Irwin N, Li YM, O'Toole JE, Benowitz LI. Mst3b, a purine-sensitive Ste20-like protein kinase, regulates axon outgrowth. Proc Natl Acad Sci USA 2006;103:18320–5.
Ishihara Y, Shimamoto N. Involvement of endonuclease G in nucleosomal DNA fragmentation under sustained endogenous oxidative stress. J Biol Chem 2006;281:6726–33.
Ito Y, Pandey P, Mishra N, Kumar S, Narula N, Kharbanda S, et al. Targeting of the c-Abl tyrosine kinase to mitochondria in endoplasmic reticulum stress-induced apoptosis. Mol Cell Biol 2001;21:6233–42.
Joza N, Susin SA, Daugas E, Stanford WL, Cho SK, Li CY, et al. Essential role of the mitochondrial apoptosis-inducing factor in programmed cell death. Nature 2001;410:549–54.
Kuwana T, Mackey MR, Perkins G, Ellisman MH, Latterich M, Schneiter R, et al. Bid, Bax, and lipids cooperate to form supramolecular openings in the outer mitochondrial membrane. Cell 2002;111:331–42.
Kyriakis JM. Signaling by the germinal center kinase family of protein kinases. J Biol Chem 1999;274:5259–62.
Lee BI, Lee DJ, Cho KJ, Kim GW. Early nuclear translocation of endonuclease G and subsequent DNA fragmentation after transient focal cerebral ischemia in mice. Neurosci Lett 2005;386:23–7.
Lee WS, Hsu CY, Wang PL, Huang CY, Chang CH, Yuan CJ. Identification and characterization of the nuclear import and export signals of the mammalian Ste20-like protein kinase 3. FEBS Lett 2004;572:41–5.
Li LY, Luo X, Wang X. Endonuclease G is an apoptotic DNase when released from mitochondria. Nature 2001;412:95–9.
Lu TJ, Lai WY, Huang CYF, Hsieh WJ, Yu JS, Hsieh YJ, et al. Inhibition of cell migration by autophosphorylated mammalian sterile 20-like kinase 3 (MST3) involves paxillin and protein-tyrosine phosphatase-PEST. J Biol Chem 2006;281:38405–17.
Luo X, Budihardjo I, Zou H, Slaughter C, Wang X. Bid, a Bcl2 interacting protein, mediates cytochrome c release from mitochondria in response to activation of cell surface death receptors. Cell 1998;94:481–90.
Martinou JC, Green DR. Breaking the mitochondrial barrier. Nat Rev Mol Cell Biol 2001;2:63–7.
Michaelson J. Cell selection in development. Biol Rev Camb Philos Soc 1987;62:115–39.
Newmeyer DD, Ferguson-Miller S. Mitochondria: releasing power for life and unleashing the machineries of death. Cell 2003;112:481–90.
Parrish J, Li L, Klotz K, Ledwich D, Wang X, Xue D. Mitochondrial endonuclease G is important for apoptosis in *C. elegans*. Nature 2001;412:90–4.
Porter AG, Urbano AGL. Does apoptosis-inducing factor (AIF) have both life and death functions in cells? BioEssays 2006;28:834–43.
Savill J, Haslett C. Granulocyte clearance by apoptosis in the resolution of inflammation. Semin Cell Biol 1995;6:385.
Schinkmann K, Blenis J. Cloning and characterization of a human STE20-like protein kinase with unusual cofactor requirements. J Biol Chem 1997;272:28695–703.
Sells MA, Chernoff J. Emerging from the Pak: the p21-activated protein kinase family. Trends Cell Biol 1997;7:162–7.
Srinivasula SM, Ahmad M, Fernandes-Alnemri T, Alnemri ES. Autoactivation of procaspase-9 by Apaf-1-mediated oligomerization. Mol Cell 1998;1:949–57.
Stegert MR, Hergovich A, Tamaskovic R, Bichsel SJ, Hemmings BA. Regulation of NDR protein kinase by hydrophobic motif phosphorylation mediated by the mammalian Ste20-like kinase MST3. Mol Cell Biol 2005;25:11019–29.
Susin SA, Lorenzo HK, Zamzami N, Marzo I, Snow BE, Brothers GM, et al. Molecular characterization of mitochondrial apoptosis-inducing factor. Nature 1999;397:441–6.
Suzuki Y, Imai Y, Nakayama H, Takahashi K, Takio K, Takahashi R. A serine protease, HtrA2, is released from the mitochondria and interacts with XIAP, inducing cell death. Mol Cell 2001;8:613–21.
Verhagen AM, Silke J, Ekert PG, Pakusch K, Kaufmann H, Connolly LM, et al. HtrA2 promotes cell death through its serine protease activity and its ability to antagonize inhibitor of apoptosis proteins. J Biol Chem 2002;277:445–54.
Vier J, Linsinger G, Häcker G. Cytochrome *c* is dispensable for fas-induced caspase activation and apoptosis. Biochem Biophys Res Commun 1999;261:71–8.
Wang X, Yang C, Chai J, Shi Y, Xue D. Mechanisms of AIF-mediated apoptotic DNA degradation in *Caenorhabditis elegans*. Science 2002;298:1587–92.
Widlak P, Li P, Wang X, Garrard WT. Cleavage preference of the apoptotic endonuclease DFF40 (caspase-activated DNase or nuclease) on naked DNA and chromatin substrates. J Biol Chem 2000;275:8226–32.
Wolter KG, Hsu YT, Smith CL, Nechushtan A, Xi XG, Youle RJ. Movement of Bax from the cytosol to mitochondria during apoptosis. J Cell Biol 1997;139:1281–92.
Wu HY, Lin CY, Lin TY, Chen TC, Yuan CJ. Mammalian Ste20-like protein kinase 3 mediates trophoblast apoptosis in spontaneous delivery. Apoptosis 2008;13:283–94.
Ye H, Cande C, Stephanou NC, Jiang S, Gurbuxani S, Larochette N, et al. DNA binding is required for the apoptogenic action of apoptosis inducing factor. Nat Struct Biol 2002;9:680–4.
Zanna C, Ghelli A, Porcelli AM, Martinuzzi A, Carelli V, Rugolo M. Caspase-independent death of Leber's hereditary optic neuropathy cybrids is driven by energetic failure and mediated by AIF and endonuclease G. Apoptosis 2005;10:997–1007.
Zhang J, Dong M, Li L, Fan Y, Pathre P, Dong J, et al. Endonuclease G is required for early embryogenesis and normal apoptosis in mice. Proc Natl Acad Sci USA 2003;100:15782–7.